Extended X-ray Absorption Fine Structure Study of Copper(I) and Copper(II) Complexes in Atom Transfer Radical Polymerization

Tomislav Pintauer,[a] Ulrich Reinöhl,[b] Martin Feth,[b] Helmut Bertagnolli,[b] and Krzysztof Matyjaszewski*[a]

Keywords: EXAFS spectroscopy / Copper / Radical reactions / Polymerizations

Extended X-ray Absorption Fine Structure (EXAFS) spectroscopy has been used to investigate structural features of Cu^{I}-Br and $Cu^{II}Br_2$ complexes with dNbpy, PMDETA, Me_6TREN, tNtpy, and Me_4CYCLAM in various solvents {dNbpy = 4,4′-bis(5-nonyl)-2,2′-bipyridine, PMDETA = *N*,*N*,*N*′,*N*′′,*N*′′-pentamethyldiethylenetriamine, Me_6TREN = tris[2-(dimethylamino)ethyl]amine, tNtpy = 4,4′,4′′-tris(5-nonyl)-2,2′:6′,2′′-terpyridine, Me_4CYCLAM = 1,4,8,11-tetramethyl-1,4,8,11-tetraazacyclotetradecane}. The structures of the Cu^{I} and Cu^{II} complexes were found to depend on the solvent polarity and the number of nitrogen atoms in the ligand. Generally, in non-polar media and with monomers typically used in ATRP, Cu^{I} complexes preferred a tetracoordinate geometry, and were either ionic as observed in $[Cu^{I}(dNbpy)_2]^+[Cu^{I}Br_2]^-$ (Cu^{I}–N_{AV} = 2.00 Å, Cu^{I}–Br_{AV} = 2.25 Å) and $[Cu^{I}(Me_4CYCLAM)]^+[Cu^{I}Br_2]^-$ (Cu^{I}–N_{AV} = 2.06 Å, Cu^{I}–Br_{AV} = 2.23 Å), or neutral as in $[Cu^{I}$(PMDETA)Br] (Cu^{I}–N_{AV} = 2.12 Å, Cu^{I}–Br_{AV} = 2.33 Å), and $[Cu^{I}$(tNtpy)Br] (Cu^{I}–N_{AV} = 2.03 Å, Cu^{I}–Br_{AV} = 2.29 Å). The EXAFS analysis of $Cu^{II}Br_2$ complexes indicated a preference for a coordination number of five, such as in $[Cu^{II}(dNbpy)_2Br]^+[Br]^-$ (Cu^{II}–N_{AV} = 2.03 Å, Cu^{II}–Br_{AV} = 2.43 Å), $[Cu^{II}(PMDETA)Br_2]$ (Cu^{II}–N_{AV} = 2.03 Å, Cu^{II}–$Br_{1,AV}$ = 2.44 Å, Cu^{II}–$Br_{2,AV}$ = 2.64 Å) and $[Cu^{II}(Me_6TREN)Br]^+[Br]^-$ (Cu^{II}–N_{AV} = 2.09 Å, Cu^{II}-Br_{AV} = 2.39 Å), with the exception of the neutral tetracoordinate $[Cu^{II}(dNbpy)Br_2]$ (Cu^{II}–N_{AV} = 2.02 Å, Cu^{II}–Br_{AV} = 2.36 Å), which has been observed in non-polar media. Additionally, polar media were found to favor bromide dissociation in $[Cu^{II}(Me_6TREN)Br]^+[Br]^-$ and $[Cu^{II}(PMDETA)Br_2]$, as indicated by a decrease in the Br and Cu coordination numbers at the Cu- and Br-*K*-edges, respectively.

Introduction and Background

The synthesis of macromolecules with well-defined compositions, architectures, and functionalities represents an ongoing effort in the field of polymer chemistry. Over the past few years, atom transfer radical polymerization (ATRP) has emerged as a very powerful and robust technique to meet these goals.[1−6] The basic working mechanism of ATRP (Scheme 1) involves a reversible switching between two oxidation states of a transition metal complex.[3,7,8] Typically, a copper(I) halide is used in conjunction with a nitrogen-based ligand (Scheme 2).[9,10]

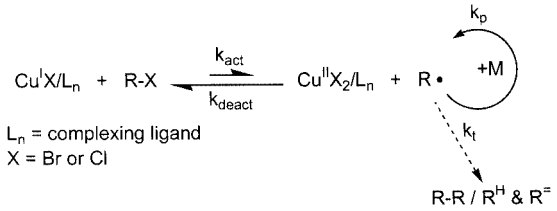

Scheme 1. Proposed mechanism for ATRP

Homolytic cleavage of the alkyl halide bond (R−X) by the Cu^{I} complex generates an alkyl radical R· and the corresponding Cu^{II} complex. The radical R· can either (a) propagate with a propagation rate constant k_p, by adding across the double bond of a vinyl monomer, (b) terminate by either coupling or disproportionation (k_t), or (c) be reversibly deactivated by the Cu^{II} complex (k_{deact}). Since the position of equilibrium is strongly shifted towards the dormant species ($k_{act} << k_{deact}$), radical termination is suppressed. As a result of the persistent radical effect,[11,12] polymers with predictable molecular weights, narrow molecular-weight distributions and high functionalities have been synthesized.[13]

Structural and mechanistic studies are crucial in understanding this mechanism further and are inherently part of the future developments of ATRP. Correlation of the catalyst structure[14−19] with reaction parameters such as the activation and deactivation rate constants[20−24] can lead to a development of more active catalysts and controlled polymerization of less reactive monomers (e.g. vinyl esters). Furthermore, systematic evaluation of the concurrent reac-

[a] Department of Chemistry, Carnegie Mellon University, 4400 Fifth Avenue, Pittsburgh, PA 15213, USA
Fax: (internat.) + 1-412/268-6897
E-mail: km3b@andrew.cmu.edu
[b] Institut für Physikalische Chemie, Universität Stuttgart, Pfaffenwaldring 55, 70569, Stuttgart, Germany
Fax: (internat.) + 49-711/685-4443
E-mail: h.bertagnolli@ipc.uni-stuttgart.de

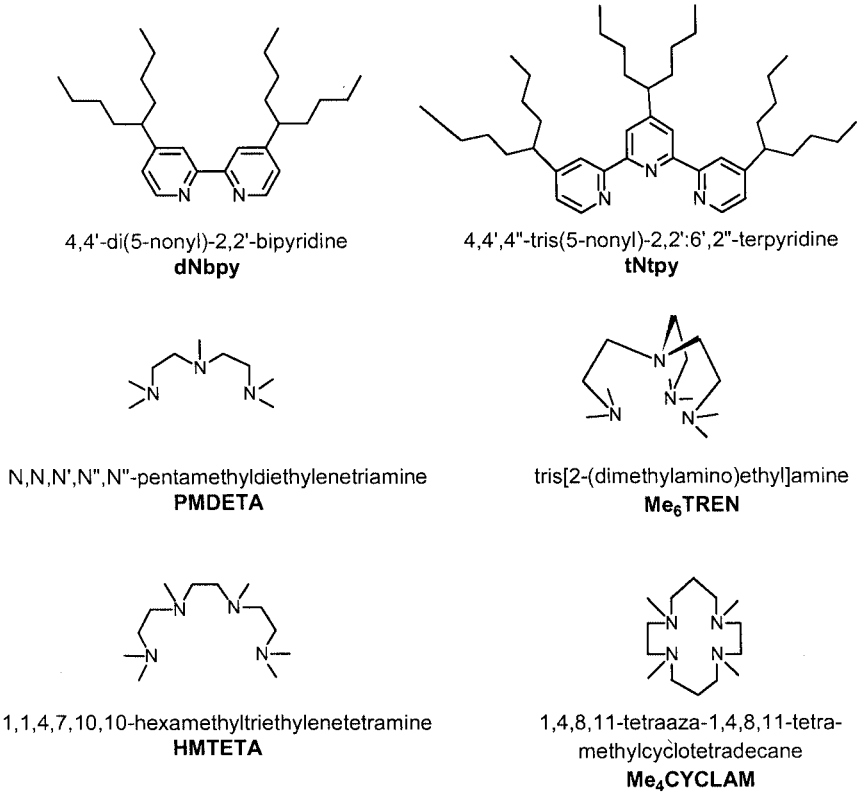

Scheme 2. Nitrogen-based ligands typically used in copper-mediated ATRP

tions that might occur in ATRP such as radical, monomer or solvent coordination[25] to the active catalysts, as well as transfer reactions associated with the ligand,[26−28] can provide much needed information about how to extend polymerization control to even higher molecular weight polymers, and generally improve the overall catalytic process.

Extended X-ray Absorption Fine Structure (EXAFS) spectroscopy has been shown to be a powerful technique for determining the structures of transition metal complexes in both the solid state and in solution.[29−32] An analysis of the EXAFS spectrum provides information on the bond lengths, the coordination number and the nature of the scattering atoms surrounding an excited atom.[33,34] In this paper, we report the results of an EXAFS spectroscopic study of $Cu^{I}Br$ and $Cu^{II}Br_2$ complexes with 4,4′-bis(5-nonyl)-2,2′-bipyridine (dNbpy), 4,4′,4′′-tris(5-nonyl)-2,2′:6′,2′′-terpyridine (tNtpy), *N*,*N*,*N*′,*N*′′,*N*′′-pentamethyldiethylenetriamine (PMDETA), tris[2-(dimethylamino)ethyl]amine (Me_6TREN) and 1,4,8,11-tetramethyl-1,4,8,11-tetraazacyclotetradecane (Me_4CYCLAM) in various solvents. The structures reported by EXAFS spectroscopy are primarily based on the interatomic distances around the absorber and their comparison with the structurally isolated and characterized model compounds. Due to the inherent errors in determination of the coordination numbers, the reported structures might also represent the average structures in solution. Therefore the possibility of the presence of other species that might co-exist in equilibrium cannot be excluded.

Results and Discussion

Model Complexes

In order to test the applicability and accuracy of EXAFS spectroscopic analysis in determining the structures of $Cu^{I}Br$ and $Cu^{II}Br_2$ complexes with nitrogen-based ligands, we have conducted measurements at Cu- and Br-*K*-edges for a series of complexes in the solid state for which the molecular structures are known. Table 1 shows the comparison between experimental bond lengths from EXAFS measurements at room temperature with distances derived from the single-crystal X-ray structures of $Cu^{I}Br$ and $Cu^{II}Br_2$ complexes with nitrogen-based ligands. Solid-state samples of $[Cu^{I}(bpy)_2]^{+}[ClO_4]^{-}$ [35] were used to model tetrahedral complexes, $[Cu^{I}(Me_6TREN)]^{+}[ClO_4]^{-}$ [36] for trigonal-bipyramidal complexes, $[Cu^{I}(bpy)Br]_2$[37] for bridged complexes, and $[N(C_4H_9)_4]^{+}[Cu^{I}Br_2]^{-}$ [38] for linear Cu^{I} complexes. Additionally, $[Cu^{II}(bpy)_2Br]^{+}[BF_4]^{-}$ [39] and $[Cu^{II}Br(Me_6TREN)]^{+}[Br]^{-}$ [40] were used as model compounds for trigonal-bipyramidal complexes, whilst $[Cu^{II}(PMDETA)Br_2]$[41] and $[Cu^{II}(terpy)Br_2]$[14,42] were used to model distorted square-pyramidal Cu^{II} complexes. As shown in Table 1, a good agreement has been observed between the distances determined by EXAFS and X-ray crystallography, confirming the accuracy of the EXAFS analysis.

The corresponding coordination numbers were also determined by iterative fitting. Typically, the error for the coordination number is about 10−15% when the peaks in the Fourier-transformed spectra are well resolved and separated

Table 1. Comparison of experimental bond lengths [Å] from EXAFS measurements at room temperature with distances in the single-crystal X-ray structures; coordination numbers were fixed to the crystallographically derived values

Complex	Cu−N_{AV} [Å] EXAFS	Cu−N_{AV} [Å] X-ray	Cu−Br_{AV} [Å] EXAFS	Cu−Br_{AV} [Å] X-ray
$[Cu^{I}(bpy)_2]^+[ClO_4]^-$ [35]	1.98	2.02		
$[Cu^{I}(Me_6TREN)]^+[ClO_4]^-$ [36]	2.13	2.16		
$[Cu^{I}(bpy)Br]_2$ [37]	2.10	2.09	2.44	2.44
			2.25	2.23
$[N(C_4H_9)_4]^+[Cu^{I}Br_2]^-$ [38]				
$[Cu^{II}(bpy)_2Br]^+[BF_4]^-$ [39]	2.01	2.04	2.41	2.42
$[Cu^{II}Br(Me_6TREN)]^+[Br]^-$ [40]	2.09	2.11	2.39	2.39
$[Cu^{II}(PMDETA)Br_2]$[41]	2.09	2.10	2.44, 2.64	2.45, 2.64
$[Cu^{II}(terpy)Br_2]$[42]	2.02	2.01	2.45	2.49

{e.g. in $[Cu^{I}(bpy)_2]^+[ClO_4]^-$ $CN(N)_{fit}$ = 3.7, r_{fit} = 1.98 Å, $CN(N)_{X\text{-}ray}$ = 4.0, $r_{X\text{-}ray}$ = 1.98 Å}. In the case of significant overlapping of the peaks, the error in the coordination number can amount to 30% {e.g. in $[Cu^{II}(bpy)_2Br]^+[BF_4]^-$ $CN(N)_{fit}$ = 2.7, r_{fit} = 2.00 Å, $CN(N)_{X\text{-}ray}$ = 4.0, $r_{X\text{-}ray}$ = 2.01 Å and $CN(Br)_{fit}$ = 0.7, r_{fit} = 2.40 Å, $CN(Br)_{X\text{-}ray}$ = 1.0, $r_{X\text{-}ray}$ = 2.41 Å}. However, the distances determined either by iterative fitting or fitting with fixed coordination numbers agree within 1% with the distances measured by X-ray crystallography. Therefore, since the error range for the coordination numbers is significantly larger than the accuracy of the distances, the interpretation of the following systems is mainly based on the determined distances and their comparison with the model compounds.

$Cu^{I}Br$ and $Cu^{II}Br_2$ Complexes with the dNbpy Ligand

Unsubstituted 2,2′-bipyridine was the first ligand used in copper-mediated ATRP.[9] Alkyl substitutions in the 4- and 4′-positions of the bipyridine ring, such as in dNbpy (Scheme 2) further improved the solubility of the catalyst in non-polar media, which resulted in higher conversions with very low polydispersities.[43] Table 2 shows the summary of room-temperature EXAFS spectroscopic measurements, in different solvents, of $Cu^{I}Br$ and $Cu^{II}Br_2$ complexes with the dNbpy ligand.

The EXAFS spectrum of the $Cu^{I}Br$ complex with 1 equiv. of dNbpy in styrene is well fit using the structural model in which the Cu^{I} center is coordinated by 3.8 nitro-

Table 2. Structural parameters of $Cu^{I}Br$ and $Cu^{II}Br_2$ complexes with dNbpy ligand, determined by EXAFS measurements under ambient conditions at the Cu- and Br-*K*-edge; MA = methyl acrylate

Complex[a]	Solvent	Backscatt.	N	*r* [Å]	σ [Å]	ΔE_0 [eV]	*k* [$Å^{-1}$]	Fit index
$Cu^{I}Br$/dNbpy	styrene	Cu−N	3.8	2.01	0.096	18.7	3.8−12.5	27.6
		Cu−Br	1.1	2.25	0.078			
		Br−Cu	0.8	2.24	0.074	21.8	4.1−12.6	27.8
	MA	Cu−N	3.7	1.99	0.100	13.6	4.0−12.5	29.6
		Cu−Br	1.3	2.26	0.090			
		Br−Cu	1.0	2.26	0.100	18.5	4.3−12.0	19.6
$Cu^{I}Br$/2dNbpy	styrene	Cu−N	2.9	2.03	0.105	19.0	4.1−12.0	36.2
		Cu−Br	1.4	2.25	0.105			
		Br−Cu	0.8	2.24	0.087	21.2	4.3−12.5	29.6
	MA	Cu−N	2.8	2.01	0.100	21.9	4.2−12.5	20.7
		Cu−Br	1.3	2.26	0.090			
		Br−Cu	0.8	2.25	0.100	14.5	4.2−12.0	34.5
$Cu^{II}Br_2$/2dNbpy	MA	Cu−N	1.4	2.01	0.071	17.2	4.0−13.7	29.1
		Cu−Br	1.5	2.37	0.071			
		Cu−C	2.0	2.94	0.049			
		Br−Cu	0.9	2.37	0.059	13.5	4.1−14.0	31.6
	toluene	Cu−N	1.8	2.03	0.051	15.0	4.1−15.1	20.1
		Cu−Br	2.1	2.37	0.074			
		Cu−C	1.6	2.93	0.049			
		Br−Cu	1.1	2.35	0.062	18.8	4.2−14.1	16.5
	MeOH	Cu−N	2.8	2.03	0.071	17.8	4.2−14.8	27.0
		Cu−Br	0.6	2.43	0.063			
		Br−Cu	0.30	2.42	0.067	19.4	4.2−14.1	56.9

[a] *N* = coordination number, *r* = absorber−backscatterer distance, σ = Debye−Waller factor. Inherent errors are approximately 10−30% for coordination numbers and Debye−Waller factors and 1% for distances.

gen atoms at a distance of 2.01 Å and 1.1 bromine atoms at a distance of 2.25 Å. The results in methyl acrylate are analogous, indicating similar structural features for the complex. Furthermore, when 2 equiv. of dNbpy were used relative to $Cu^{I}Br$, the average $Cu^{I}-N$ and $Cu^{I}-Br$ distances did not change significantly, although the coordination number of nitrogen appears to be lower than in solutions that contained only 1 equiv. of dNbpy. Taking into account the inherent error of 10−30% for the coordination numbers and 1% for the distances, the most plausible species in non-polar media is the ionic complex $[Cu^{I}(dNbpy)_2]^+[Cu^{I}Br_2]^-$. The neutral complex $[Cu^{I}(dNbpy)Br]_2$ can be ruled out since $Cu^{I}-Br$ bond lengths in Br-bridged Cu^{I} complexes are typically 2.4−2.5 Å (Table 1).[37] The average $Cu^{I}-N$ bond length in the $[Cu^{I}(dNbpy)_2]^+$ cation (2.01 Å) is consistent with the average $Cu^{I}-N$ bond lengths in bpy derivatives such as $[Cu^{I}(bpy)_2]^+[ClO_4]^-$ [35] (2.021 Å), $[Cu^{I}(6,6'\text{-}Me_2\text{-}bpy)_2]^+[BF_4]^-$ [44] (2.032 Å) and $[Cu^{I}(4,4'\text{-}Me_2\text{-}bpy)_2]^+[Br]^-$ [45] (2.035 Å). Furthermore, the $Cu^{I}-Br$ bond length in the linear $[Cu^{I}Br_2]^-$ anion (2.25 Å) is similar to that seen in related complexes such as $[N(C_4H_9)_4]^+[Cu^{I}Br_2]^-$ [38] (2.226 Å), $[P(C_6H_5)_4]^+[Cu^{I}Br_2]^-$ [46] (2.214 Å) and $[Cu^{I}(phen)_2]^+[Cu^{I}Br_2]^-$ [47] (2.216 Å).

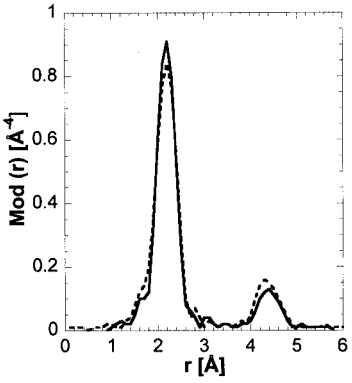

Figure 1. Comparison of the experimental Fourier transformed $k^3\chi(k)$ functions at the Br-*K*-edge of $Cu^{I}Br$/dNbpy in toluene (solid line) and $[N(C_4H_9)_4][Cu^{I}Br_2]$ in the solid state (broken lines)

Figure 1 shows the Fourier transformations of the EXAFS functions at the Br-*K*-edge of the $Cu^{I}Br$/2dNbpy complex in toluene and of $[N(C_4H_9)_4]^+[Cu^{I}Br_2]^-$ in the solid state. The similarity of the two spectra further suggests the presence of $[Cu^{I}Br_2]^-$ anions in the $Cu^{I}Br$/(2)dNbpy complex in non-polar media, which is consistent with the proposed species $[Cu^{I}(dNbpy)_2]^+[Cu^{I}Br_2]^-$.

We have investigated the complexation between $Cu^{I}Br$ and dNbpy in non-polar media previously by Electrospray Ionization Mass Spectrometry (ESI-MS)[48] and EXAFS spectroscopy.[15] ESI-MS spectra of $Cu^{I}Br$ complexed with 1 or 2 equiv. of dNbpy in toluene, methyl acrylate, or styrene showed only the presence of the $[Cu^{I}(dNbpy)_2]^+$ cation and the $[Cu^{I}Br_2]^-$ anion, which is consistent with the proposed species, $[Cu^{I}(dNbpy)_2]^+[Cu^{I}Br_2]^-$. Furthermore, the EXAFS analysis at the Cu-*K*-edge also indicated the presence of $[Cu^{I}(dNbpy)_2]^+[Cu^{I}Br_2]^-$. Recently, the molecular structure of a related bpy-based ATRP active catalyst, $[Cu^{I}(dNEObpy)_2]^+[Cu^{I}Br_2]^-$ (dNEObpy = 4,4′-bis{[dimethyl(neophyl)silyl]methyl}-2,2′-bipyridine) further confirmed this unusual 1:1 stoichiometry in non-polar media between $Cu^{I}Br$ and bpy based ligands.[17]

Taking into account the inherent error in determining the coordination numbers by EXAFS spectroscopy (10−30%), $[Cu^{I}(dNbpy)_2]^+[Cu^{I}Br_2]^-$ might not be the only complex present in solution. Consequently, the possibility of more than one species co-existing in equilibrium cannot be excluded. Depending on the temperature, solvent polarity, and the amount of dNbpy, the substitution of Br in $[Cu^{I}Br_2]^-$ by dNbpy may lead to the formation of $[Cu^{I}(dNbpy)_2]^+[Br]^-$ (Scheme 3).

A similar equilibrium has been proposed earlier for $[Cu^{I}(dNEObpy)_2]^+[Cu^{I}Br_2]^-$.[17] Additionally, solvent and monomer coordination to the Cu^{I} center[49] cannot be ruled out due to the limited sensitivity of EXAFS measurements.[32] More experimental evidence is therefore needed to further characterize this system.

The results of the EXAFS spectroscopic analysis of the $Cu^{II}Br_2$ complex with 2 equiv. of dNbpy in methyl acrylate (Table 2) indicate that the coordination sphere around the Cu^{II} center consists of 1.4 N atoms at a distance of 2.01 Å and 1.5 Br atoms at a distance of 2.37 Å (a carbon backscatterer was used in the analysis in order to increase the accuracy of the fit). In toluene, the average $Cu^{II}-N$ and $Cu^{II}-Br$ distances did not change significantly, but the coordination numbers of N and Br increased to 1.8 and 2.1, respectively. In a more polar solvent, such as methanol, the coordination number of N increased even further to 2.8, and that of Br decreased to 0.6. Furthermore, the decrease

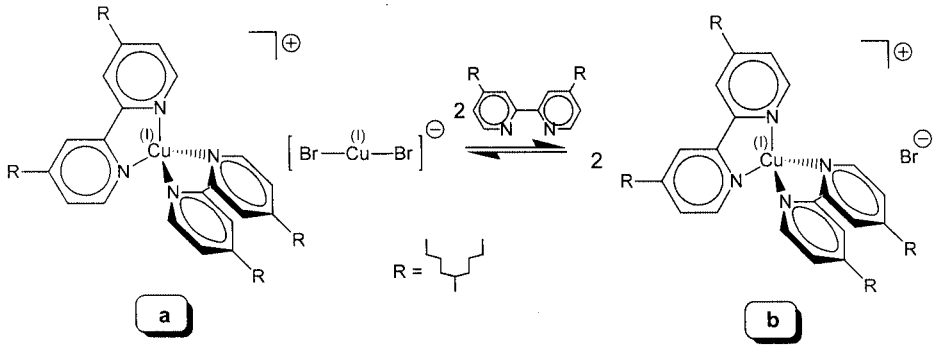

Scheme 3. Proposed structures for the $Cu^{I}Br$/(2)dNbpy complex in (a) non-polar and (b) polar media

in the Br coordination number was accompanied by an increase in the average $Cu^{II}-Br$ bond length from 2.37 to 2.43 Å. In non-polar media such as toluene and methyl acrylate, the results of the EXAFS spectroscopic measurements are consistent with the neutral complex $[Cu^{I}-{}^{I}(dNbpy)Br_2]$ which has been isolated and characterized previously.[16] In the solid state, $[Cu^{II}(dNbpy)Br_2]$ has a distorted square-planar geometry. The Cu^{II} center is coordinated by the two nitrogen atoms of a single dNbpy ligand ($Cu^{II}-N_{AV}$ = 2.017 Å) and to two bromine atoms ($Cu^{II}-Br_{AV}$ = 2.359 Å). $[Cu^{II}(dNbpy)Br_2]$ undergoes bromide substitution by dNbpy to form the ionic complex $[Cu^{II}(dNbpy)_2Br]^+[Br]^-$, which is strongly favored a in more polar medium such as methanol (Scheme 4).

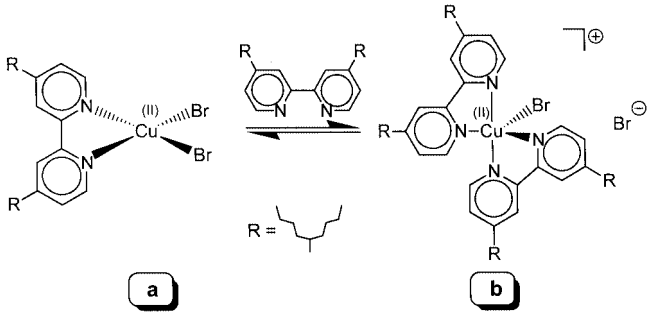

Scheme 4. Proposed structures for the $Cu^{II}Br_2$/(2)dNbpy complex in (a) non-polar and (b) polar media based on EXAFS measurements

The average $Cu^{II}-N$ (2.03 Å) and $Cu^{II}-Br$ (2.43 Å) bond lengths of $[Cu^{II}(dNbpy)_2Br]^+[Br]^-$ in methanol, as determined by EXAFS, are in good agreement with the average distances in the structurally characterized compounds $[Cu^{II}(bpy)_2Br]^+[Br]^-$ [50] ($Cu^{II}-N_{AV}$ = 2.034 Å, $Cu^{II}-Br$ = 2.429 Å), $[Cu^{II}(bpy)_2Br]^+[PF_6]^-$ [39] ($Cu^{II}-N_{AV}$ = 2.044 Å, $Cu^{II}-Br$ = 2.467 Å) and $[Cu^{II}(dNbpy)_2Br]^+[Cu^{I}Br_2]^-$ [14] ($Cu^{II}-N_{AV}$ = 2.016 Å, $Cu^{II}-Br$ = 2.426 Å). Additionally, as ΔH and ΔS for the equilibrium reaction in Scheme 4 were found to be negative, an increase in the temperature favors formation of the neutral complex $[Cu^{II}(dNbpy)Br_2]$. It was determined that under the typical initial reverse ATRP conditions [$T \geq 90$ °C and total copper(II) concentration in the range 1.0×10^{-2} to 1.0×10^{-1} M], the $Cu^{I}-{}^{I}Br_2$ complex and 2 equiv. of dNbpy will predominantly form the neutral complex $[Cu^{II}(dNbpy)Br_2]$.[16]

We have previously investigated the complexation between $Cu^{II}Br_2$ and dNbpy in non-polar media, including monomers that are typically used in ATRP. Based on the EXAFS[15] and ESI-MS[48] study, we proposed the formation of a 1:1 complex, $[Cu^{II}(dNbpy)_2Br]^+[Cu^{II}Br_3]^-$. The structure was primarily based on the relative intensities of the absorbance peaks in the ESI-MS spectra since both species have, on average, the same atomic distances as derived from the EXAFS measurements. The absence of the charge in $[Cu^{II}(dNbpy)Br_2]$ may be responsible for its weak intensity. This could consequently lead to the wrong conclusion about the most probable structure in solution.

Table 3. Structural parameters of $Cu^{I}Br$ and $Cu^{II}Br_2$ complexes with PMDETA ligand, determined by EXAFS measurements under ambient conditions at the Cu- and Br-*K*-edge

Complex[a]	Solvent	Backscatt.	N	*r* [Å]	σ [Å]	ΔE_0 [eV]	*k* [$Å^{-1}$]	Fit index
$Cu^{I}Br$/PMDETA	MA	Cu−N	2.9	2.12	0.114	15.6	4.3−13.6	15.7
		Cu−Br	1.2	2.33	0.084			
		Cu−C	5.1	2.94	0.120			
		Br−Cu	1.0	2.32	0.063	19.1	4.2−14.1	19.6
	styrene	Cu−N	2.7	2.14	0.109	14.5	4.4−13.6	11.4
		Cu−Br	1.2	2.33	0.089			
		Cu−C	5.9	2.97	0.118			
		Br−Cu	1.0	2.33	0.063	19.1	4.2−14.1	19.6
	toluene	Cu−N	2.5	2.10	0.097	19.0	4.5−13.6	27.7
		Cu−Br	1.0	2.30	0.091			
		Cu−C	6.2	2.91	0.116			
		Br−Cu	1.3	2.29	0.097	24.7	4.4−14.9	25.6
	MeOH	Cu−N	2.8	2.13	0.105	15.6	4.4−14.0	21.4
		Cu−Br	1.1	2.35	0.095			
		Cu−C	6.0	2.94	0.118			
		Br−Cu	1.0	2.33	0.093	23.0	4.2−14.4	24.7
$Cu^{II}Br_2$/PMDETA	toluene/	Cu−N	3.6	2.13	0.099	12.5	4.4−14.0	29.1
	MeOH	Cu−Br	1.0	2.42	0.084			
	(4:1 vol.)	Cu−C	7.4	2.99	0.107			
		Br−Cu	0.5	2.39	0.074	20.7	4.2−12.0	27.0
	MeOH	Cu−N	3.1	2.09	0.087	16.5	3.8−15.0	23.3
		Cu−Br	1.1	2.41	0.087			
		Cu−C	7.0	2.94	0.107			
		Br−Cu	0.4	2.39	0.077	13.2	3.8−12.0	21.7
	H_2O	Cu−N	4.0	2.06	0.081	15.3	3.9−14.8	40.9
		Cu−C	6.0	2.91	0.093			

[a] *N* = coordination number, *r* = absorber−backscatterer distance, σ = Debye−Waller factor. Inherent errors are approximately 10−30% for coordination numbers and Debye−Waller factors and 1% for distances.

$Cu^{I}Br$ and $Cu^{II}Br_2$ Complexes with the PMDETA Ligand

Apart from substituted bipyridines, other linear and cyclic amines were successfully used as ligands in the formation of ATRP catalysts.[51−55] In particular, commercially available tridentate PMDETA (Scheme 2) showed a high potential for the controlled polymerization of a variety of monomers. Typically, the ligand/copper(I) halide ratio used in the polymerization was 1:1. Shown in Table 3 is a summary of the room-temperature EXAFS measurements of $Cu^{I}Br$ and $Cu^{II}Br_2$ complexes with 1 equiv. of PMDETA in different solvents, including monomers typically used in ATRP. The typical experimental and calculated Fourier transformations of the EXAFS spectra for the $Cu^{I}Br$/PMDETA and $Cu^{II}Br_2$/PMDETA complexes are shown in Figures 2 and 3, respectively.

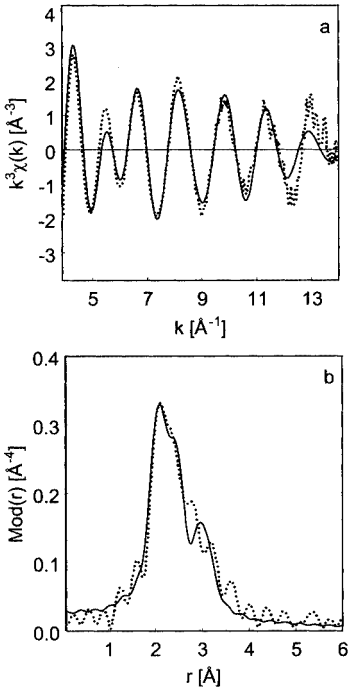

Figure 2. Experimental (dotted line) and calculated (solid line) $k^3\chi(k)$ functions (a) (k range: 3.90−14.0 Å^{-1}) and their Fourier transformations (b) at the Cu-K-edge for $Cu^{I}Br$/PMDETA in toluene at room temperature (see Table 3 for fit parameters)

The results of the EXAFS spectroscopic analysis of $Cu^{I}Br$/PMDETA in methyl acrylate, styrene, toluene, and methanol (Table 3) indicate similar structural features for the complex in these solvents. In all solvents, the EXAFS data are well fit by a structural model that includes 3.0 nitrogen atoms at a distance of 2.12 Å and 1.0 bromine atoms at a distance of 2.33 Å.

The average $Cu^{I}-N$ bond length is in agreement with those in other Cu^{I} complexes with similar nitrogen-based chromophores.[56] Additionally, the $Cu^{I}-Br$ bond length indicates covalent bonding to the Cu^{I} center. Based on these results, one structure that is consistent with the EXAFS analysis is the neutral complex [Cu^{I}(PMDETA)Br]. However, other structures might also co-exist in equilibrium and are shown in Scheme 5.

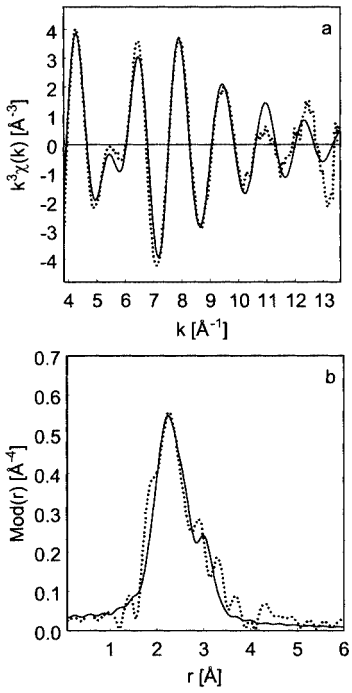

Figure 3. Experimental (dotted line) and calculated (solid line) $k^3\chi(k)$ functions (a) (k range: 3.80−14.1 Å^{-1}) and their Fourier transformations (b) at the Cu-K-edge for $Cu^{II}Br_2$/PMDETA in toluene/methanol mixture (80%/20% v/v) at room temperature (see Table 3 for fit parameters)

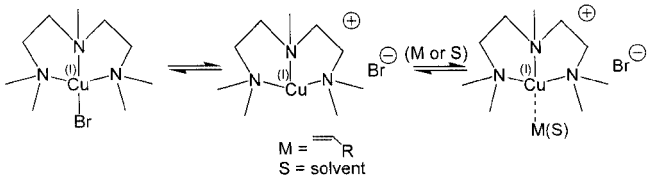

Scheme 5. Proposed structures for the $Cu^{I}Br$/PMDETA complex

Based on the solvent polarity and temperature, the dissociation of bromide could lead to the formation of the ionic complex [Cu^{I}(PMDETA)]$^+$[Br]$^-$. The coordinatively unsaturated [Cu^{I}(PMDETA)]$^+$ cation can be further coordinated by solvent (S) or monomer leading to the formation of [Cu^{I}(PMDETA)(S)]$^+$[Br]$^-$ and [Cu^{I}(PMDETA)(M)]$^+$[Br]$^-$, respectively. We were recently able to isolate and structurally characterize [Cu^{I}(PMDETA)(π-styrene)]$^+$[BPh_4]$^-$ and [Cu^{I}(PMDETA)(π-MA)]$^+$[BPh_4]$^-$ which model the monomer coordination to [Cu^{I}(PMDETA)]$^+$.[57] The monomer coordination occurred via π-bond formation, with a significant contribution from Cu^{I} π-back donation, as manifested in the strong shielding of the vinyl protons. Similar coordination has also been observed previously in [Cu^{I}(dien)(π-1-hexene)]$^+$[BPh_4]$^-$ (dien = diethylenetriamine).[58] A more detailed characterization of the $Cu^{I}Br$/PMDETA catalytic system in ATRP is under investigation.

Room temperature EXAFS measurements of the $Cu^{II}Br_2$ complex with 1 equiv. of PMDETA are shown in Table 3. The study was limited to relatively polar media, due to the poor solubility of the complex in typical non-polar ATRP solutions.

In a toluene/MeOH mixture (4:1 vol.), the EXAFS spectrum was fit reasonably well by assuming that the Cu^{II} center is coordinated by 3.6 nitrogen atoms at a distance of 2.13 Å and 1.0 bromine atoms at a distance of 2.42 Å. In more polar methanol, the average $Cu^{II}-N$ and $Cu^{II}-Br$ bond lengths did not change significantly. On the other hand, the EXAFS spectrum in H_2O indicated the absence of a $Cu^{II}-Br$ bond, which was also confirmed by measurements at the Br-*K*-edge. The structure of the $Cu^{II}Br_2$ complex with 1 equiv. of PMDETA has been recently reported. In the solid state, the complex exists as $[Cu^{II}(PMDETA)Br_2]$ with a distorted square-pyramidal coordination sphere.[14] The Cu^{II} center is coordinated by three nitrogen atoms of the PMDETA ligand ($Cu^{II}-N_{AV}$ = 2.098 Å) and two bromine atoms ($Cu^{II}-Br_{AV}$ = 2.545 Å). The $Cu^{II}-Br$ bond length in the apical position (2.644 Å) is much longer than the $Cu^{II}-Br$ bond length in the basal position (2.446 Å). This was attributed to the relatively small energy differences between the trigonal bipyramidal and square-pyramidal geometries of pentacoordinate Cu^{II} complexes. The average $Cu^{II}-N$ bond lengths determined by EXAFS spectroscopy in toluene/MeOH (2.13 Å), MeOH (2.09 Å) and H_2O (2.06 Å) are in good agreement with the average $Cu^{II}-N$ bond length in $[Cu^{II}(PMDETA)Br_2]$ (2.098 Å). However, the average $Cu^{II}-Br$ bond lengths in toluene/MeOH (2.42 Å) and MeOH (2.41 Å) are inconsistent with the average bond length in $[Cu^{II}(PMDETA)Br_2]$ (2.545 Å). Taking into account the coordination number of Br at the Cu- and Br-*K*-edges, the structural features of the $Cu^{II}Br_2$ complex with PMDETA determined by EXAFS can be explained in terms of bromide dissociation from $[Cu^{II}(PMDETA)Br_2]$. In toluene/MeOH and MeOH, the EXAFS data suggest the presence of $[Cu^{II}(PMDETA)Br]^+[Br]^+$. In H_2O, additional dissociation of bromide could result in the formation of $[Cu^{II}(PMDETA)]^{2+}[Br]_2^-$. Since Cu^{II} complexes prefer a pentacoordinate geometry,[56] the vacant coordination sites in $[Cu^{II}(PMDETA)Br]^+[Br]^-$ and $[Cu^{II}(PMDETA)]^{2+}[Br]_2^-$ are likely to be occupied by solvent molecules (MeOH or H_2O) (Scheme 6).

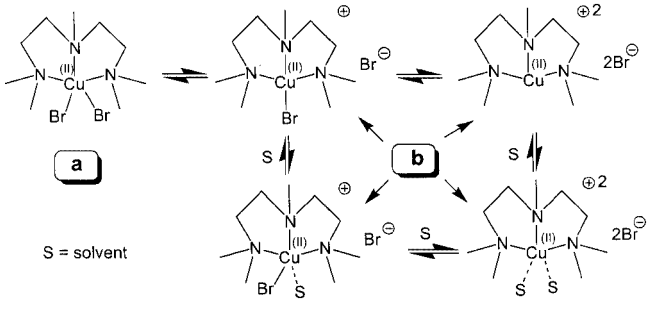

Scheme 6. Proposed structures for the $Cu^{II}Br_2$/PMDETA complex in (a) non-polar and (b) polar media based on EXAFS measurements

This has been demonstrated in the solid state with X-ray studies of the structures of the related complexes $[Cu^{II}(PMDETA)(H_2O)]^{2+}[ClO_4]_2^-$ [59] and $[Cu^{II}(PMDETA)(H_2O)_2]^{2+}[BF_4]_2^-$.[60] The replacement of bromide via π-bond formation with a monomer is less likely to occur with Cu^{II} complexes because the binding constants are typically very low.[61] However, substitution can potentially occur with functionalized olefins because they can additionally coordinate to the Cu^{II} complexes via functional groups (S, O, N etc.).[62]

Dissociation of halide anions from Cu^{II} complexes has been the subject of numerous investigations.[63–65] The equilibrium constants were found to strongly depend on the temperature and polarity of the reaction medium. Furthermore, polar and protic solvents such as MeOH and H_2O were found to favor halide anions dissociation, an observation which was most likely due to solvation effects. High values of the equilibrium constant for halide dissociation from $[Cu^{II}(L)-X]^+$ (X = Br^- or Cl^-) complexes could explain the fast ATRP reactions in polar media. The halide dissociation from $[Cu^{II}(L)-X]^+$ shifts the position of the ATRP equilibrium (see Scheme 1), resulting in an increase in radical concentration. Our recent measurements determined that the equilibrium constant for bromide dissociation from $[Cu^{II}(PMDETA)Br_2]$ in H_2O at room temperature was K = 0.18 mol·L^{-1}.[66] Using this value, one can estimate that under typical conditions of the EXAFS experiment (room temperature, $[Cu^{II}Br_2]_0$ = $[PMDETA]_0 \approx 0.05$ M) approximately 80% of the $Cu^{II}Br_2$/PMDETA complex in H_2O contains dissociated bromide anions. This further supports the results of the EXAFS analysis and structures proposed in Scheme 6. A more detailed study of the effect of halide dissociation from other ATRP active Cu^{II} complexes is currently being carried out.

$Cu^{I}Br$ and $Cu^{II}Br_2$ Complexes with the Me_6TREN Ligands

Tris[2-(dimethylamino)ethyl]amine (Me_6TREN, Scheme 2) is a tetradentate nitrogen-based ligand that has been successfully used in ATRP. Typically, the ligand/$Cu^{I}Br$ ratio was 1:1. This catalytic system showed a very high activity, enabling fast and controlled polymerization of methyl acrylate at ambient temperature.[52] The results of EXAFS measurements of $Cu^{I}Br$ and $Cu^{II}Br_2$ complexes with Me_6TREN in different solvents are summarized in Table 4.

The Cu-*K*-edge EXAFS spectrum of the $Cu^{I}Br$ complex with 1 equiv. of Me_6TREN in styrene can be best modeled by assuming that the coordination sphere around the Cu^{I} center is occupied by 3.0 nitrogen atoms at a distance of 2.15 Å and 1.2 bromine atoms at a distance of 2.33 Å. The results in methyl acrylate and toluene (Figure 4) are analogous, indicating similar structural features of the complex in those solvents.

Taking into account the 18-electron rule and the tetradentate nature of Me_6TREN, one would expect that the most probable structure of the $Cu^{I}Br/Me_6TREN$ complex in solution would be $[Cu^{I}(Me_6TREN)]^+[Br]^-$. The average $Cu^{I}-N$ bond lengths in styrene (2.15 Å), methyl acrylate (2.15 Å) and toluene (2.14 Å) are in agreement with the

Table 4. Structural parameters of $Cu^{I}Br$ and $Cu^{II}Br_2$ complexes with Me_6TREN ligand, determined by EXAFS measurements under ambient conditions at the Cu- and Br-*K*-edge; MA = methyl acrylate

Complex[a]	Solvent	Backscatt.	N	*r* [Å]	σ [Å]	ΔE_0 [eV]	*k* [$Å^{-1}$]	Fit index
$Cu^{I}Br/Me_6TREN$	styrene	Cu−N	3.0	2.15	0.114	14.8	4.2−15.6	15.4
		Cu−Br	1.2	2.33	0.080			
		Cu−C	4.0	2.95	0.105			
		Br−Cu	1.0	2.32	0.071	19.1	3.6−14.0	17.1
	MA	Cu−N	2.8	2.15	0.110	15.3	4.2−15.4	12.3
		Cu−Br	1.1	2.33	0.077			
		Cu−C	5.9	2.94	0.116			
		Br−Cu	1.0	2.32	0.077	18.6	4.2−13.1	14.6
	toluene	Cu−N	2.8	2.14	0.100	18.6	4.2−14.6	20.8
		Cu−Br	1.3	2.31	0.084			
		Cu−C	5.4	2.91	0.118			
		Br−Cu	1.2	2.31	0.086	21.8	3.8−14.0	18.0
$Cu^{II}Br_2/Me_6TREN$	MeOH	Cu−N	3.2	2.13	0.100	18.8	4.2−15.0	19.9
		Cu−Br	1.4	2.38	0.081			
		Cu−C	8.7	2.94	0.114			
		Br−Cu	0.9	2.38	0.087	14.8	4.1−14.4	32.0
	H_2O	Cu−N	4.1	2.06	0.105	21.1	4.4−13.0	31.4
		Cu−Br	0.30	2.42	0.074			
		Cu−C	8.0	2.89	0.105			
		Br−Cu	0.0					

[a] *N* = coordination number, *r* = absorber−backscatterer distance, σ = Debye−Waller factor. Inherent errors are approximately 10−30% for coordination numbers and Debye−Waller factors and 1% for distances.

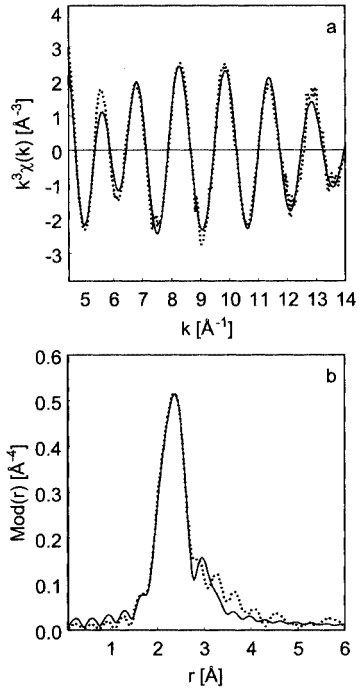

Figure 4. Experimental (dotted line) and calculated (solid line) $k^3\chi(k)$ functions (a) (*k* range: 4.20−14.6 $Å^{-1}$) and their Fourier transformations (b) at the Cu-*K*-edge for $Cu^{I}Br/Me_6TREN$ in toluene at room temperature (see Table 4 for fit parameters)

previously characterized complex $[Cu^{I}(Me_6TREN)]^{+}$-$[ClO_4]^{-}$ (2.161 Å).[36] However, the coordination number of N appears to be rather low for the tetradentate Me_6TREN ligand. Additionally, the presence of a Br backscatterer in the spectrum of the Cu-*K*-edge indicates covalent bonding to the Cu^{I} center. This evidence contradicts the presence of the solely ionic species $[Cu^{I}(Me_6TREN)]^{+}[Br]^{-}$.

The presence of a Cu^{I}−Br absorbance in the EXAFS spectrum of $Cu^{I}Br/Me_6TREN$ could suggest the presence of linear $[Cu^{I}Br_2]^{-}$ anions, as described earlier in the case of $[Cu^{I}(dNbpy)_2]^{+}[Cu^{I}Br_2]^{-}$. However, the average Cu^{I}−Br bond lengths in styrene (2.33 Å), methyl acrylate (2.33 Å), and toluene (2.31 Å) appear to be longer than the Cu^{I}−Br bond length in other Cu^{I} complexes with $[Cu^{I}Br_2]^{-}$ anions (2.206−2.232 Å).[17,38,46,47] The elongation of the Cu^{I}−Br bond in $[Cu^{I}Br_2]^{-}$ anions is possible, but was not observed in the structurally related complex $[Cu^{I}(HMTETA)]^{+}[Cu^{I}Cl_2]^{-}$ (HMTETA = 1,1,4,7,10,10-hexamethyltriethylenetetramine), in which the Cu^{I}−Cl bond length was found to be similar to those seen in other Cu^{I} complexes with linear $[Cu^{I}Cl_2]^{-}$ anions.[36]

The structure of the $Cu^{I}Br/Me_6TREN$ complex consistent with the EXAFS analysis is likeley to be the neutral $[Cu^{I}(Me_6TREN')Br]$ (Me_6TREN' denotes a tricoordinate Me_6TREN). Similar structures were proposed earlier for copper[67] and cobalt[68] complexes with the Me_6TREN ligand in order to explain the kinetics of ligand substitution reactions. Furthermore, the dissociation of one "amine" arm in Cu^{II} complexes with other tetradentate nitrogen-based ligands has also been reported.[69,70]

Due to the sensitivity of EXAFS measurements, inherent errors in coordination numbers (10−30%), and also the possibility of the co-existence of more than one species in equilibrium means that all complexes discussed above could be present in solution. The proposed structures are shown in Scheme 7. More experimental evidence is needed to confirm the proposed structures, relative proportions of each species and more importantly their activity in the $Cu^{I}Br/Me_6TREN$ catalytic system in ATRP.

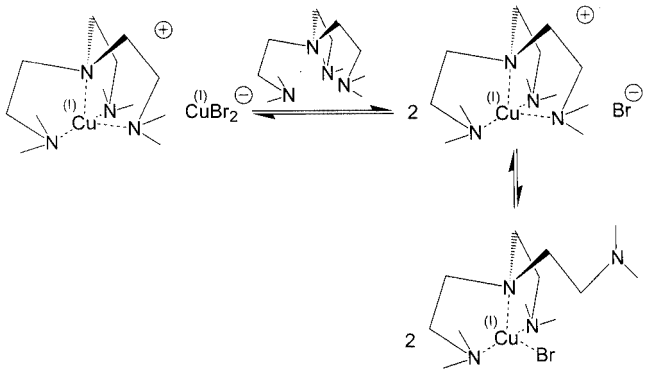

Scheme 7. Proposed structures for the $Cu^{I}Br/Me_6TREN$ complex

Room-temperature EXAFS data for the $Cu^{II}Br_2$ complex with 1 equiv. of Me_6TREN are summarized in Table 4. In methanol, the EXAFS spectrum of the Cu-*K*-edge (Figure 5) was reasonably well fit using the structural model that includes 3.2 nitrogen atoms at a distance of 2.13 Å and 1.4 bromine atoms at a distance of 2.38 Å. These data are consistent with $[Cu^{II}(Me_6TREN)Br]^+[Br]^-$ which was isolated and characterized previously.[40] $[Cu^{II}(Me_6TREN)Br]^+[Br]^-$ has a distorted trigonal-bipyramidal geometry. The Cu^{II} center is coordinated by 4 nitrogen atoms of the Me_6TREN ligand ($Cu^{II}-N_{AV}$ = 2.116 Å) and 1 bromine atom ($Cu^{II}-Br$ = 2.393 Å). As indicated in Table 4, there is a significant decrease in the coordination number of Br in the more polar H_2O. This result points to the bromide dissociation as discussed previously in the case

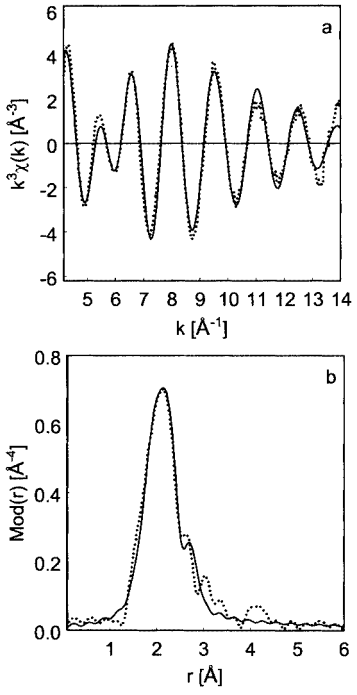

Figure 5. Experimental (dotted line) and calculated (solid line) $k^3\chi(k)$ functions (a) (k range: 4.00−14.2 $Å^{-1}$) and their Fourier transformations (b) at the Cu-*K*-edge for $Cu^{II}Br_2/Me_6TREN$ in methanol at room temperature (see Table 4 for fit parameters)

of $[Cu^{II}(PMDETA)Br_2]$. The proposed equilibrium is shown in Scheme 8.

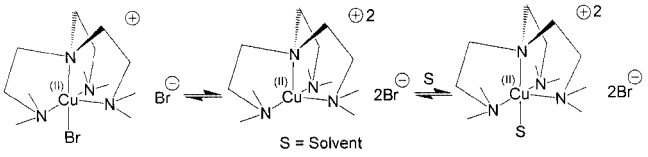

Scheme 8. Proposed structures for the $Cu^{II}Br_2/Me_6TREN$ complex

The vacant coordination site in $[Cu^{II}(Me_6TREN)]^{2+}[Br]_2^-$ is most likely occupied by the solvent molecule (H_2O or MeOH), as demonstrated in the structurally related complex $[Cu^{II}(Me_6TREN)(H_2O)]^{2+}[ClO_4]_2^-$.[70] The equilibrium constant for the dissociation of Br^- from the $[Cu^{II}(Me_6TREN)Br]^+$ chromophore has been determined spectrophotometrically in H_2O.[63,64] Under typical EXAFS conditions ($[Cu^{II}Br_2]_0$ = $[Me_6TREN]_0$ = 0.05 M), the equilibrium constant of 0.23 $mol\cdot L^{-1}$ would indicate that approximately 85% of the complex has dissociated with formation of bromide anions. This further supports the results of the EXAFS analysis and structures proposed in Scheme 8.

$Cu^{I}Br$ Complexes with the $Me_4CYCLAM$ and tNtpy Ligands

The substituted terpyridine (tNtpy)[71] and cyclic tetradentate amine ($Me_4CYCLAM$)[52] were also used in the ATRP of various monomers (Scheme 2). The polymerization of methyl acrylate and styrene catalyzed by $Cu^{I}Br$/tNtpy was controlled and the resultant polymers had relatively low polydispersities (M_w/M_n < 1.2). ATRP using $Cu^{I}Br/Me_4CYCLAM$ resulted in fast and uncontrolled polymerizations, which was attributed to a low deactivation rate constant.[14,72,73] Table 5 shows the summary of EXAFS-determined structural data for $Cu^{I}Br$ complexes with the tNtpy and $Me_4CYCLAM$ ligands.

The Cu-*K*-edge EXAFS spectrum of the $Cu^{I}Br/Me_4CYCLAM$ complex in methyl acrylate (Figure 6) is well fit using the structural model in which Cu^{I} is coordinated by 3.8 nitrogen atoms at a distance of 2.06 Å and 1.7 bromine atoms at a distance of 2.23 Å. In a more polar medium (MA/MeOH = 3:1, v/v), the signal due to the coordinated bromine atoms disappears and only nitrogen backscatterers are visible in the FT Cu-*K*-edge EXAFS spectrum. The average $Cu^{I}-N$ bond lengths for the $Cu^{I}Br/Me_4CYCLAM$ complex in methyl acrylate (2.06 Å) and methyl acrylate/MeOH (3:1, v/v) (2.05 Å) are shorter than the average $Cu^{I}-N$ bond lengths in the related complexes $[Cu^{I}(HMTETA)]^+[Cu^{I}Cl_2]^-$ ($Cu^{I}-N_{AV}$ = 2.111 Å)[36] and $[Cu^{I}(Me_6TREN)]^+[ClO_4]^-$ ($Cu^{I}-N_{AV}$ = 2.161 Å).[74] The shortening of the average $Cu^{I}-N$ bond length in $Cu^{I}Br/Me_4CYCLAM$ could be due to the steric strain imposed by the cyclic $Me_4CYCLAM$ ligand as described in the literature.[75,76] Copper(I) complexes with $Me_4CYCLAM$ are therefore expected to adopt a square-planar geometry as

Table 5. Structural parameters of $Cu^{I}Br$ complexes with Me_4CYCLAM and tNtpy ligands, determined by EXAFS measurements under ambient conditions at the Cu- and Br-*K*-edge; MA = methyl acrylate

Complex[a]	Solvent	Backscatt.	N	*r* [Å]	σ [Å]	ΔE_0 [eV]	*k* [$Å^{-1}$]	Fit index
$Cu^{I}Br$/	MA	Cu−N	3.8	2.06	0.112	17.0	4.2−11.6	49.7
		Cu−Br	1.7	2.23	0.114			
		Cu−C	4.1	2.93	0.114			
Me_4cyclam	MA/	Cu−N	4.1	2.05	0.093	16.4	4.2−13.4	37.3
	MeOH	Cu−C	3.0	2.83	0.104			
	(3:1 vol.)	Cu−C	4.0	3.44	0.094			
		Cu−Br	0.0					
$Cu^{I}Br$/tNtpy	MA	Cu−N	2.7	2.03	0.099	12.6	3.9−14.9	32.9
		Cu−Br	1.0	2.29	0.101			
		Cu−C	3.1	2.94	0.102			
	styrene	Cu−N	2.6	2.03	0.114	17.6	4.0−11.1	27.6
		Cu−Br	0.7	2.29	0.081			
		Cu−C	2.9	2.96	0.102			
		Br−Cu	0.9	2.29	0.102			

[a] *N* = coordination number, *r* = absorber−backscatterer distance, σ = Debye−Waller factor. Inherent errors are approximately 10−30% for coordination numbers and Debye−Waller factors and 1% for distances.

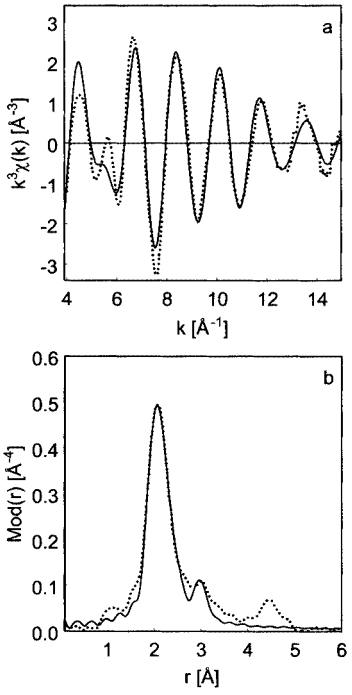

Figure 6. Experimental (dotted line) and calculated (solid line) $k^3\chi(k)$ functions (a) (*k* range: 3.90−14.9 $Å^{-1}$) and their Fourier transformations (b) at the Cu-*K*-edge for $Cu^{I}Br$/Me_4CYCLAM in methyl acrylate at room temperature (see Table 5 for fit parameters)

opposed to tetrahedral and square-pyramidal structures observed in $[Cu^{I}(HMTETA)]^{+}[Cu^{I}Cl_2]^{-}$ and $[Cu^{I}(Me_6TREN)]^{+}[ClO_4]^{-}$, respectively. The average $Cu^{I}-Br$ bond length and coordination number of Br in $Cu^{I}Br$/Me_4CYCLAM in methyl acrylate are consistent with Cu^{I} complexes containing $[Cu^{I}Br_2]^{-}$ anions (2.206−2.232 Å).[17,38,46,47] Similar to $Cu^{I}Br$/Me_6TREN discussed earlier, the EXAFS results of $Cu^{I}Br$/Me_4CYCLAM in methyl acrylate are consistent with $[Cu^{I}(Me_4CYCLAM)]^{+}[Cu^{I}Br_2]^{-}$. In more polar media, the complex predominantly exists as $[Cu^{I}(Me_4CYCLAM)]^{+}[Br]^{-}$ (Scheme 9). The 1:1/2 stoichiometry in $[Cu^{I}(Me_4CYCLAM)]^{+}[Cu^{I}Br_2]^{-}$ indicates the presence of free Me_4CYCLAM in the ATRP system since the catalyst is typically prepared by mixing $Cu^{I}Br$ with an equimolar amount of Me_4CYCLAM. Consequently, the free ligand can participate in chain transfer reactions which limit the control of the polymerization at higher molecular weights, as observed previously in the case of PMDETA.[26,27]

The EXAFS-determined structural data of the $Cu^{I}Br$ complex with tNtpy (Table 5) in methyl acrylate indicate that the coordination sphere around the Cu^{I} center is occupied by 2.7 nitrogen atoms at a distance of 2.03 Å and 1.0 bromine atoms at a distance of 2.29 Å. The coordination numbers and distances in styrene indicate similar structural features of the complex. The EXAFS data in methyl acrylate and styrene are consistent with the neutral complex $[Cu^{I}(tNtpy)Br]$. However, as discussed earlier in the case of the $Cu^{I}Br$ complex with tridentate PMDETA, other species might co-exist in equilibrium. The proposed structures are shown in Scheme 9, and are subject to further investigation.

The structures of the $Cu^{II}Br_2$ complexes with tNtpy and Me_4CYCLAM in solution, although not investigated by EXAFS, are expected to be similar to the complexes with PMDETA and Me_6TREN as discussed above. In the solid state, the $Cu^{II}Br_2$ complex with tNtpy exists as neutral $[Cu^{II}(tNtpy)Br_2]$.[14] The Cu^{II} center has a distorted square-bipyramidal geometry and is coordinated by 3 nitrogen atoms of the tNtpy ligand ($Cu^{II}-N_{AV}$ = 2.027 Å) and 2 bromine atoms ($Cu^{II}-Br_{AV}$ = 2.467 Å). Analogous to the molecular structure of $[Cu^{II}(PMDETA)Br_2]$, the $Cu^{II}-Br$ bond in the apical position (2.528 Å) was found to be longer than the $Cu^{II}-Br$ bond in the basal position (2.407 Å). Moreover, the $Cu^{II}Br_2$ complex with Me_4CYCLAM has been isolated as ionic $[Cu^{II}(Me_4CYCLAM)Br]^{+}[Br]^{-}$.[14] The Cu^{II} center in the complex is distorted square-pyramidal with the average $Cu^{II}-N$ and $Cu^{II}-Br$ bond lengths

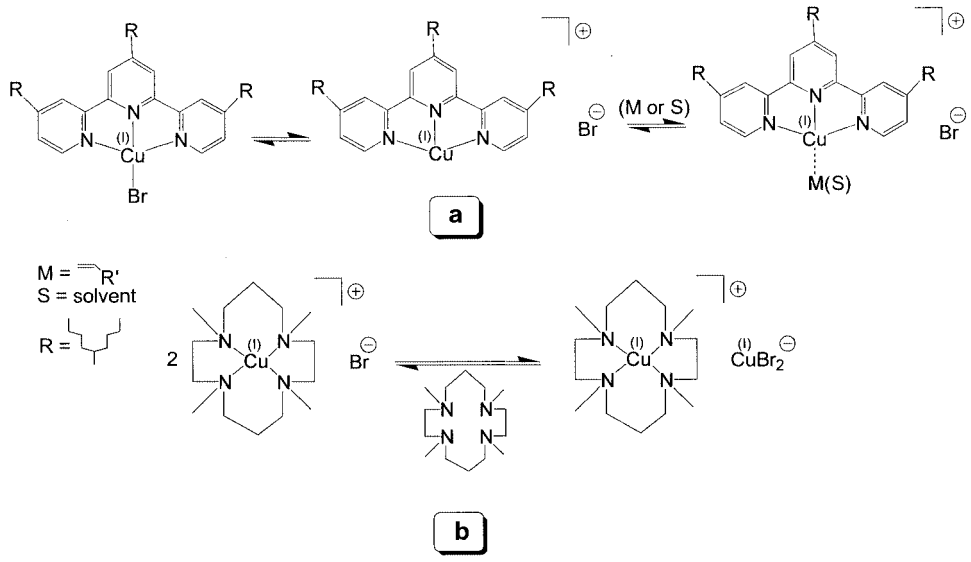

Scheme 9. Proposed structures for the (a) Cu^IBr/tNtpy and (b) $Cu^IBr/Me_4CYCLAM$ complexes

being 2.087 and 2.809 Å, respectively. The complex is expected to undergo bromide substitution in polar media such as H_2O and MeOH, similar to the previously discussed PMDETA- and Me_6TREN-based complexes.

Conclusions

In summary, EXAFS has been used to investigate the structural features of Cu^IBr and $Cu^{II}Br_2$ complexes with dNbpy, PMDETA, Me_6TREN, tNtpy, and Me_4CYCLAM in various solvents, including styrene and methyl acrylate which are monomers typically used in ATRP. The structures reported by EXAFS were primarily based on the interatomic distances around the absorber, due to the inherent error in the coordination numbers. In non-polar media, the EXAFS spectroscopic analysis of the Cu^IBr complex with dNbpy at room temperature indicated the presence of $[Cu^I(dNbpy)_2]^+[Cu^IBr_2]^-$ {Cu^I-N_{AV} = 2.01 Å (styrene), 1.99 Å (MA), Cu^I-Br_{AV} = 2.25 Å (styrene), 2.26 Å (MA)}. In polar media, such as MeOH, $[Cu^I(dNbpy)_2]^+[Br]^-$ was the preferred species (Cu^I-N_{AV} = 2.01 Å). Similarly, the EXAFS spectra of the $Cu^{II}Br_2$ complex of dNbpy in nonpolar and polar media were consistent with the presence of $[Cu^{II}(dNbpy)Br_2]$ {$Cu^{II}-N_{AV}$ = 2.01 Å (MA), 2.03 Å (toluene), $Cu^{II}-Br_{AV}$ = 2.37 Å (MA), 2.37 Å (toluene)} and $[Cu^{II}(dNbpy)_2Br]^+[Br]^-$ {$Cu^{II}-N_{AV}$ = 2.03 Å (MeOH), $Cu^{II}-Br_{AV}$ = 2.43 Å (MeOH)}, respectively. The EXAFS-determined structural data of Cu^IBr complexes with the tridentate ligands PMDETA and tNtpy in methyl acrylate indicated the presence of neutral $[Cu^I(PMDETA)Br]$ (Cu^I-N_{AV} = 2.12 Å, Cu^I-Br_{AV} = 2.33 Å) and $[Cu^I(tNtpy)Br]$ (Cu^I-N_{AV} = 2.03 Å, Cu^I-Br_{AV} = 2.29 Å), respectively. The coordination numbers and distances indicated similar structural features to those of the complexes in toluene and styrene. The results of the EXAFS analysis of the Cu^IBr/Me_6TREN complex in methyl acrylate, styrene, and toluene were well fit by a structural model that included 3 nitrogen atoms at a distance of 2.15 Å and 1 bromine atom at 2.32 Å, which potentially indicated the presence of several species namely $[Cu^I(Me_6TREN)]^+[Br]^-$, $[Cu^I(Me_6TREN)]^+[Cu^IBr_2]^-$, and $[Cu^I(Me_6TREN')Br]$ (Me_6TREN' denotes a tricoordinate Me_6TREN). The decrease in the coordination number of N was not observed in the Cu^IBr complex with tetradentate Me_4CYCLAM, which in a non-polar medium such as methyl acrylate, predominantly exist as $[Cu^I(Me_4CYCLAM)]^+[Cu^IBr_2]^-$ (Cu^I-N_{AV} = 2.06 Å, Cu^I-Br_{AV} = 2.23 Å). In more polar media, the structure changed to $[Cu^I(Me_4CYCLAM)]^+[Br]^-$ (Cu^I-N_{AV} = 2.05 Å). Additionally, the $Cu^{II}Br_2$ complexes with PMDETA and Me_6TREN, namely $[Cu^{II}(PMDETA)Br_2]$ ($Cu^{II}-N_{AV}$ = 2.09 Å, $Cu^{II}-Br_{1,AV}$ = 2.44 Å, $Cu^{II}-Br_{2,AV}$ = 2.64 Å) and $[Cu^{II}(Me_6TREN)Br]^+[Br]^-$ ($Cu^{II}-N_{AV}$ = 2.09 Å, $Cu^{II}-Br_{AV}$ = 2.39 Å), respectively, were found to undergo bromide dissociation in MeOH and H_2O, as indicated by a decrease in the Br/Cu coordination number the latter being determined by analysis of the EXAFS spectra at the Cu- and Br-*K*-edges.

Experimental Section

Materials: Cu^IBr (99.999%), $Cu^{II}Br_2$ (99.999%), $Cu^{II}(CF_3SO_3)_2$ (99%), and $[N(C_4H_9)_4]^+[Br]^-$ (98%) were purchased from Aldrich and used as received. *N,N,N′,N″,N″*-Pentamethyldiethylenetriamine (PMDETA) (99%, Aldrich) was distilled under nitrogen. 2,2′-Bipyridine (99%, Aldrich) was recrystallized from methanol. Tris[2-(dimethylamino)ethyl]amine (Me_6TREN)[77] and 4,4′-bis(5-nonyl)-2,2′-bipyridine (dNbpy)[78] were prepared according to literature procedures. All solvents were distilled and deoxygenated prior to use. Unless otherwise noted, experiments were performed under nitrogen in a dry box or using a Schlenk line. Elemental analyses for C, H, and N were performed by Chemisar Laboratories Inc., Guelph, Ontario, Canada.

Model Compounds: $[Cu^{I}(bpy)_2]^+[ClO_4]^-$,[35] $[Cu^{I}(bpy)Br_2]$,[37] $[N(C_4H_9)_4]^+[Cu^{I}Br_2]^-$,[38] $[Cu^{II}(terpy)Br_2]$,[14,42] $[Cu^{II}(Me_6TREN)Br]^+[Br]^-$,[40] $[Cu^{II}(PMDETA)Br_2]$,[41] and $[Cu^{II}(dNbpy)Br_2]$[16] were synthesized according to literature procedures. $[Cu^{II}(dNbpy)_2Br]^+[Y]^-$ (Y = Br^-, PF_6^-, and $CF_3SO_3^-$) were prepared in CH_3CN according to the procedures for $[Cu^{II}(bpy)_2Br]^+[Br]^-$,[50] $[Cu^{II}(bpy)_2Br]^+[PF_6]^-$,[39] and $[Cu^{II}(bpy)_2Br]^+[CF_3SO_3]^-$ [79] but using dNbpy instead of bpy.

EXAFS Measurements and Data Analysis: The EXAFS measurements of the samples were performed at the beamline 2−3 at the SSRL, a division of SLAC, which is operated by Stanford University (USA). For the measurements at the Cu- *K*-edge (8982.5 eV) and Br-*K*-edge (13474.0 eV) an Si(111) double crystal monochromator was used. A synchrotron beam current up to 100 mA was used (electron energy 3.00 GeV). All experiments were carried out under ambient conditions. The tilt of the second monochromator crystal was set to 30% harmonic rejection. Energy resolution was estimated to be about 2 eV for the Cu-*K*-edge and 4 eV for the Br-*K*-edge. Data were collected in transmission mode with ion chambers. All ion chambers were filled with nitrogen in the case of the measurements at the Cu-*K*-edge, and the second and third chamber with argon in the case of the measurements at the Br-*K*-edge. Energy calibration was performed with the corresponding metal foils in the case of Cu, and lead metal foil (Pb L_{III}-edge) in the case of Br. The samples in the solid state were embedded in a polyethylene matrix and pressed into pellets. Liquid samples were measured in a specially designed transmission sample cell for liquids which was filled under nitrogen. The concentration of all samples was adjusted to yield an absorption jump of $\Delta\mu \approx 1.5$. Data evaluation started with background absorption removal from the experimental absorption spectrum by subtraction of a Victoreen-type polynomial. The background-subtracted spectrum was then convoluted with a series of increasingly broader Gauss functions and the common intersection point of the convoluted spectra was taken as the energy E_0.[80,81] To determine the smooth part of the spectrum, corrected for pre-edge absorption, a piecewise polynomial was used. It was adjusted in such a manner that the low-*R* components of the resultant Fourier transformation were minimal. After division of the background-subtracted spectrum by its smooth part, the photon energy was converted into photoelectron wave numbers *k*. The resultant EXAFS function was weighted with k^3. Data analysis in *k* space was performed according to the curved wave multiple scattering formalism of the program EXCURV92 with XALPHA phase and amplitude functions.[82] The mean free path of the scattered electrons was calculated from the imaginary part of the potential (VPI was set to −4.00) and an overall energy shift (ΔE_0) was assumed. The Amplitude Reduction Factor (AFAC) was set to a value of 0.8 in the case of the Cu-*K*-edge as well as the Br-*K*-edge. The fitting of the spectra at the Cu-*K*-edge was typically performed by using Br and N backscatterers. For some complexes, a C backscatterer was also used in order to improve the accuracy of the fit.

Acknowledgments

Financial support from the CMU CRP Consortium and an NSF grant (CHE-0096601) is greatly appreciated. The authors also acknowledge the SSRL for the kind support of synchrotron radiation facilities.

[1] K. Matyjaszewski (Ed.), *Controlled Radical Polymerization*, vol. 685, ACS Symposium Series, Washington, DC, **1998**.
[2] K. Matyjaszewski (Ed.), *Controlled/Living Radical Polymerization: Progress in ATRP, NMP and RAFT*, vol. 768, ACS Symposium Series, Washington, DC, **2000**.
[3] K. Matyjaszewski, J. Xia, *Chem. Rev.* **2001**, *101*, 2921−2990.
[4] M. Kamigaito, T. Ando, M. Sawamoto, *Chem. Rev.* **2001**, *101*, 3689−3745.
[5] K. Matyjaszewski, T. P. Davis, *Handbook of Radical Polymerization*, John Wiley & Sons, Inc., Hoboken, **2002**.
[6] M. Qinggao, K. L. Wooley, *J. Polym. Sci. Part A: Polym. Chem.* **2000**, *38*, 4805−4820.
[7] K. Matyjaszewski, *Chem. Eur. J.* **1999**, *5*, 3095−3102.
[8] T. E. Patten, K. Matyjaszewski, *Acc. Chem. Res.* **1999**, *32*, 895−903.
[9] J.-S. Wang, K. Matyjaszewski, *J. Am. Chem. Soc.* **1995**, *117*, 5614−5615.
[10] T. E. Patten, J. Xia, T. Abernathy, K. Matyjaszewski, *Science* **1996**, *272*, 866−868.
[11] H. Fischer, *Chem. Rev.* **2001**, *101*, 3581−3610.
[12] H. Fischer, *J. Polym. Sci. Part A: Polym. Chem.* **1999**, *37*, 1885−1901.
[13] V. Coessens, T. Pintauer, K. Matyjaszewski, *Prog. Polym. Sci.* **2001**, *26*, 337−377.
[14] G. Kickelbick, T. Pintauer, K. Matyjaszewski, *New. J. Chem.* **2002**, *26*, 462−468.
[15] G. Kickelbick, U. Reinohl, T. S. Ertel, A. Weber, H. Bertagnolli, K. Matyjaszewski, *Inorg. Chem.* **2001**, *40*, 6−8.
[16] T. Pintauer, J. Qiu, G. Kickelbick, K. Matyjaszewski, *Inorg. Chem.* **2001**, *40*, 2818−2824.
[17] A. T. Levy, M. M. Olmstead, T. E. Patten, *Inorg. Chem.* **2000**, *39*, 1628−1634.
[18] D. M. Haddleton, A. J. Clark, D. J. Duncalf, A. M. Heming, D. Kukulj, A. J. Shooter, *J. Chem. Soc., Dalton Trans.* **1998**, 381−385.
[19] D. M. Haddleton, D. J. Duncalf, D. Kukulj, M. C. Crossman, S. G. Jackson, S. A. F. Bon, A. J. Clark, A. J. Shooter, *Eur. J. Inorg. Chem.* **1998**, 1799−1806.
[20] K. Matyjaszewski, H.-j. Paik, P. Zhou, S. J. Diamanti, *Macromolecules* **2001**, *34*, 5125−5131.
[21] A. Goto, T. Fukuda, *Macromol. Rapid Commun.* **1999**, *20*, 633−636.
[22] K. Ohno, A. Goto, T. Fukuda, J. Xia, K. Matyjaszewski, *Macromolecules* **1998**, *31*, 2699−2701.
[23] K. Matyjaszewski, *J. Macromol. Sci., Pure Appl. Chem.* **1997**, *A34*, 1785−1801.
[24] T. Pintauer, P. Zhou, K. Matyjaszewski, *J. Am. Chem. Soc.* **2002**, *124*, 8196−8197.
[25] D. M. Haddleton, S. Perrier, S. A. F. Bon, *Macromolecules* **2000**, *33*, 8246−8251.
[26] F. Schon, M. Hartenstein, A. H. E. Muller, *Macromolecules* **2001**, *34*, 5394−5397.
[27] M. Bednarek, T. Biedron, P. Kubisa, *Macromol. Chem. Phys.* **2000**, *201*, 58−66.
[28] K. Matyjaszewski, K. A. Davis, T. E. Patten, M. Wei, *Tetrahedron* **1997**, *53*, 15321−15329.
[29] P. A. Lee, P. Citrin, P. Eisenberger, B. M. Kincaid, *Rev. Mod. Phys.* **1980**, *53*, 769−806.
[30] H. Bertagnolli, T. S. Ertel, *Angew. Chem. Int. Ed. Engl.* **1994**, *33*, 45−66.
[31] B. K. Teo, *Acc. Chem. Res.* **1980**, *13*, 412−419.
[32] J. E. Penner-Hahn, *Coord. Chem. Rev.* **1999**, *190−192*, 1101−1123.
[33] E. A. Stern, *Phys. Rev. B* **1974**, *10*, 3027−3037.
[34] F. W. Lytle, D. E. Sayers, E. A. Stern, *Phys. Rev. B* **1975**, *11*, 4825−4835.
[35] M. Munakata, S. Kitagawa, A. Asahara, H. Masuda, *Bull. Chem. Soc. Jpn.* **1987**, *60*, 1927−1929.
[36] M. Becker, F. W. Heinemann, F. Knoch, W. Donaubauer, G.

Liehr, S. Schindler, G. Golub, H. Cohen, D. Meyerstein, *Eur. J. Inorg. Chem.* **2000**, 719−726.
[37] B. W. Skelton, A. F. Waters, A. H. White, *Aust. J. Chem.* **1991**, *44*, 1207−1215.
[38] M. Asplund, S. Jagner, M. Nilsson, *Acta Chem. Scand., Ser. A* **1983**, *37*, 57−62.
[39] R. J. Crutchley, R. Hynes, E. J. Gabe, *Inorg. Chem.* **1990**, *29*, 4921−4928.
[40] M. D. Vaira, P. L. Orioli, *Acta Crystallogr., Sect. B* **1968**, *24*, 595−599.
[41] S. R. Breeze, S. Wang, *Inorg. Chem.* **1996**, *35*, 3404−3408.
[42] M. I. Arriortua, J. L. Mesa, T. Rojo, T. Debaerdemaeker, D. Beltran-Porter, H. Stratemeier, D. Reinen, *Inorg. Chem.* **1988**, *27*, 2976−2981.
[43] K. Matyjaszewski, T. E. Patten, J. Xia, *J. Am. Chem. Soc.* **1997**, *119*, 674−680.
[44] P. J. Burke, D. R. McMillin, W. R. Robinson, *Inorg. Chem.* **1980**, *19*, 1211−1214.
[45] R. D. Willett, G. Pon, C. Nagy, *Inorg. Chem.* **2001**, *40*, 4342−4352.
[46] S. Anderson, S. Jagner, *Acta Chem. Scand., Ser. A* **1985**, *39*, 297−305.
[47] P. C. Healy, L. M. Engelhardt, V. A. Patrick, A. H. White, *J. Chem. Soc., Dalton Trans.* **1985**, 2541−2545.
[48] T. Pintauer, C. B. Jasieczek, K. Matyjaszewski, *J. Mass. Spectrom.* **2000**, *35*, 1295−1299.
[49] H. Masuda, K. Machida, *J. Chem. Soc., Dalton Trans.* **1988**, 1907−1910.
[50] M. A. Khan, D. G. Tuck, *Acta Crystallogr., Sect. B* **1981**, *B37*, 1409−1412.
[51] J. Xia, K. Matyjaszewski, *Macromolecules* **1997**, *30*, 7697−7700.
[52] J. Xia, S. G. Gaynor, K. Matyjaszewski, *Macromolecules* **1998**, *31*, 5958−5959.
[53] J. Xia, K. Matyjaszewski, *Macromolecules* **1999**, *32*, 2434−2437.
[54] J. Xia, X. Zhang, K. Matyjaszewski, in: *Transition Metal Catalysis in Macromolecular Design*, vol. 760 (Eds.: L. S. Boffa, B. M. Novak), Am. Chem. Soc., Washington, D. C., **2000**, pp. 207−223.
[55] K. Matyjaszewski, B. Gobelt, H. Paik, C. P. Horwitz, *Macromolecules* **2001**, *34*, 430−440.
[56] G. Wilkinson, *Comprehensive Coordination Chemistry*, Pergamon Press, New York, **1987**, vol. 5, pp. 539−551.
[57] T. Pintauer, N. V. Tsarevsky, G. Kickelbick, K. Matyjaszewski, *Polym. Prepr. (Am. Chem. Soc., Div. Polym. Chem.)* **2002**, *43*, 221−222.
[58] M. Pasquali, C. Floriani, A. Gaetani-Manfredotti, A. Chiesi-Villa, *Inorg. Chem.* **1979**, *18*, 3535−3542.
[59] M. J. Scott, R. H. Holm, *J. Am. Chem. Soc.* **1994**, *116*, 11357−11376.
[60] S. J. Barlow, S. J. Hill, J. E. Hocking, P. Hubberstey, W.-S. Li, *J. Chem. Soc., Dalton Trans.* **1997**, *24*, 4701−4704.
[61] F. R. Hartley, *Chem. Rev.* **1973**, *73*, 163−190.
[62] R. Jones, *Chem. Rev.* **1968**, *68*, 785−807.
[63] G. Golub, A. Lashaz, H. Cohen, P. Paoletti, A. Bencini, B. Valtancoli, D. Meyerstein, *Inorg. Chim. Acta* **1997**, *255*, 111−115.
[64] G. Golub, H. Cohen, P. Paoletti, A. Bencini, L. Messori, I. Bertini, D. Meyerstein, *J. Am. Chem. Soc.* **1995**, *117*, 8353−8361.
[65] S.-J. Ishiguro, L. Nagy, H. Ohtaki, *Bull. Chem. Soc. Jpn.* **1987**, *60*, 2053−2058.
[66] T. Pintauer, B. McKenzie, K. Matyjaszewski, *Polym. Prepr. (Am. Chem. Soc., Div. Polym. Chem.)* **2002**, *43*, 217−218.
[67] F. Thaler, C. D. Hubbard, F. W. Heinemann, R. Eldik, S. Schindler, I. Fabian, A. M. Dittler-Klingemann, F. E. Hahn, C. Orvig, *Inorg. Chem.* **1998**, *37*, 4022−4029.
[68] Z.-L. Lu, M. S. A. Hamza, R. Eldik, *Eur. J. Inorg. Chem.* **2001**, 503−510.
[69] J. H. Coates, P. R. Collins, S. F. Lincoln, *J. Chem. Soc., Faraday Trans.* **1979**, *75*, 1236−1244.
[70] J. H. Coates, P. R. Collins, S. F. Lincoln, *Aust. J. Chem.* **1980**, *33*, 1381−1387.
[71] G. Kickelbick, K. Matyjaszewski, *Macromol. Rapid Commun.* **1999**, *20*, 341−346.
[72] J. Gromada, K. Matyjaszewski, *Macromolecules* **2001**, *34*, 7664−7671.
[73] J. Gromada, K. Matyjaszewski, *Macromolecules* **2002**, *35*, 6167−6173.
[74] M. Becker, F. W. Heinemann, S. Schindler, *Chem. Eur. J.* **1999**, *5*, 3124−3129.
[75] M. Pasquali, C. Floriani, G. Venturi, A. G. Mandredotti, A. Chiesi-Villa, *J. Am. Chem. Soc.* **1982**, *104*, 4092−4099.
[76] L. M. Engelhardt, R. A. Papsergio, A. H. White, *Aust. J. Chem.* **1984**, *37*, 2207−2213.
[77] M. Ciampolini, N. Nardi, *Inorg. Chem.* **1966**, *5*, 41−44.
[78] T. B. Hadda, H. L. Bozec, *Polyhedron* **1988**, *7*, 575−577.
[79] C. O′Sullivan, G. Murphy, B. Murphy, B. Hathaway, *J. Chem. Soc., Dalton Trans.* **1999**, *11*, 1835−1844.
[80] T. S. Ertel, H. Bertagnolli, S. Huckmann, U. Kolb, D. Peter, *Appl. Spectrosc.* **1992**, *46*, 690−698.
[81] M. Newville, P. Livins, Y. Yakoby, J. J. Rehr, E. A. Stern, *Phys. Rev. B: Condens. Matter Mater. Phys.* **1993**, *47*, 14126−14131.
[82] S. J. Gurman, N. Binsted, I. Ross, *J. Phys. C* **1984**, *17*, 143−151.

Received September 5, 2002

